Monthly Notices of the ROYAL ASTRONOMICAL SOCIETY

Mon. Not. R. Astron. Soc. **419,** 3028–3038 (2012) doi:10.1111/j.1365-2966.2011.19939.x

Kepler observations of the high-amplitude δ Scuti star V2367 Cyg

L. A. Balona,[1★] P. Lenz,[2] V. Antoci,[3] S. Bernabei,[4] G. Catanzaro,[5] J. Daszyńska-Daszkiewicz,[6] M. Di Criscienzo,[7] A. Grigahcène,[8] G. Handler,[2] D. W. Kurtz,[9] M. Marconi,[10] J. Molenda-Żakowicz,[6] A. Moya,[11] J. M. Nemec,[12] A. Pigulski,[6] D. Pricopi,[13] V. Ripepi,[10] B. Smalley,[14] J. C. Suárez,[15] M. Suran,[13] J. R. Hall,[16] K. Kinemuchi[16]† and T. C. Klaus[16]

[1]*South African Astronomical Observatory, PO Box 9, Observatory 7935, Cape Town, South Africa*
[2]*Copernicus Astronomical Center, Bartycka 18, 00-716 Warsaw, Poland*
[3]*Institute of Astronomy, University of Vienna, Türkenschanzstr. 18, A-1180 Vienna, Austria*
[4]*INAF-Osservatorio Astronomico di Bologna, Via Ranzani 1, I-40127 Bologna, Italy*
[5]*INAF-Osservatorio Astrofisico di Catania, Via S. Sofia 78, I-95123 Catania, Italy*
[6]*Instytut Astronomiczny, Uniwersytet Wrocławski, Kopernika 11, 51-622 Wrocław, Poland*
[7]*INAF-Osservatorio Astronomico di Roma, via di Frascati 33, 00040 Monteporzio, Roma, Italy*
[8]*Centro de Astrofísica, Faculdade de Ciencias, Universidade do Porto, Rua das Estrelas, 4150-762 Porto, Portugal*
[9]*Jeremiah Horrocks Institute, University of Central Lancashire, Preston PR1 2HE*
[10]*INAF-Osservatorio Astronomico di Capodimonte, Via Moiariello 16, I-80131 Napoli, Italy*
[11]*Departamento de Astrofísica, ESAC Campus, PO Box 78, 28691 Villanueva de la Cañada, Madrid, Spain*
[12]*Department of Physics & Astronomy, Camosun College, Victoria, British Columbia V8P 5J2, Canada*
[13]*Astronomical Institute of the Romanian Academy, Bucharest, Romania*
[14]*Astrophysics Group, Keele University, Staffordshire ST5 5BG*
[15]*Instituto de Astrofísica de Andalucía (CSIC), CP3004 Granada, Spain*
[16]*Orbital Sciences Corporation/NASA Ames Research Center, Moffett Field, CA 94035, USA*

Accepted 2011 October 3. Received 2011 October 3; in original form 2011 August 10

ABSTRACT

We analyse *Kepler* observations of the high-amplitude δ Scuti (HADS) star V2367 Cyg (KIC 9408694). The variations are dominated by a mode with frequency $f_1 = 5.6611\,\mathrm{d}^{-1}$. Two other independent modes with $f_2 = 7.1490\,\mathrm{d}^{-1}$ and $f_3 = 7.7756\,\mathrm{d}^{-1}$ have amplitudes an order of magnitude smaller than f_1. Nearly all the light variation is due to these three modes and their combination frequencies, but several hundred other frequencies of very low amplitude are also present. The amplitudes of the principal modes may vary slightly with time. The star has twice the projected rotational velocity of any other HADS star, which makes it unusual. We find a correlation between the phases of the combination frequencies and their pulsation frequencies, which is not understood. Since modes of highest amplitude in HADS stars are normally radial modes, we assumed that this would also be true in this star. However, attempts to model the observed frequencies as radial modes without mode interaction were not successful. For a star with such a relatively high rotational velocity, it is important to consider the effect of mode interaction. Indeed, when this was done, we were able to obtain a model in which a good match with f_1 and f_2 is obtained, with f_1 being the fundamental radial mode.

Key words: stars: individual: V2367 Cyg – stars: oscillations – stars: variables: δ Scuti.

1 INTRODUCTION

The *Kepler* mission is designed to detect earth-like planets around solar-type stars by the transit method (Koch et al. 2010). *Kepler* has measured the brightness of over 100 000 stars in a 105-deg^2 fixed field of view with unprecedented precision. Among these are a large number of δ Scuti (δ Sct) stars, including V2367 Cyg (KIC 9408694, where KIC = Kepler Input Catalog, Brown et al. 2011).

High-amplitude δ Scuti (HADS) stars (previously known as dwarf Cepheids or AI Vel stars) are commonly defined as δ Sct stars with peak-to-peak light amplitudes in excess of 0.3 mag. From the ground, HADS stars typically have only one or two dominant frequencies which are most probably radial modes. Some stars,

†Name corrected after online publication 2011 December 16.
★E-mail: lab@saao.ac.za

© 2011 The Authors
Monthly Notices of the Royal Astronomical Society © 2011 RAS

Downloaded from http://mnras.oxfordjournals.org/ by guest on March 17, 2016

for example, AI Vel (Walraven, Walraven & Balona 1992), RY Lep (Rodríguez et al. 2004; Derekas et al. 2009) and V974 Oph (Poretti 2003), appear to have low-amplitude non-radial modes in addition to the dominant radial mode(s). Recently, a HADS star observed by the *CoRoT* spacecraft was discovered to have many non-radial modes as well as small but very clear amplitude modulation of the fundamental radial mode (Poretti et al. 2011).

HADS stars seem to be concentrated in the central part of the instability strip in a well-defined region. Fewer than 1 per cent of the stars that lie in the δ Sct region are HADS stars (Lee et al. 2008). There is no sharp distinction between HADS and other δ Sct stars; whenever a HADS star is observed in more detail, non-radial modes become detectable, making the star resemble an ordinary δ Sct star. The distinction is mostly in the large light amplitude, which one may expect of radial modes. Some HADS stars are members of spectroscopic binaries (Derekas et al. 2009).

HADS stars are slow rotators ($v \sin i < 30\,\mathrm{km\,s^{-1}}$) and intermediate between δ Sct stars and classical Cepheids in pulsational behaviour (Breger 2007). In fact, first-overtone classical Cepheids and HADS stars follow the same period–luminosity relation with no discontinuity. The distinction between the two groups is arbitrary (Soszynski et al. 2008). In the interior of a giant star, even high-frequency p modes behave like high-order g modes. The large number of spatial oscillations of these modes in the deep interior of giant stars lead to severe radiative damping. As a result, non-radial modes are increasingly damped for more massive δ Sct stars, which explains why HADS stars pulsate in mostly radial modes and why in the even more massive classical Cepheids, non-radial modes are no longer visible (Dziembowski 1977). This may not be the only reason, or even the correct reason, why low-degree non-radial modes are damped in giant stars and the problem needs further investigation (Mulet-Marquis et al. 2007).

Because damping of non-radial modes increases as the star evolves, one may expect that in the more evolved δ Sct stars radial modes start to dominate. In fact, ground-based observations of HADS stars suggest that there is a group of these stars which pulsate just in the fundamental and first-overtone modes and with no non-radial modes (Poretti et al. 2005). Of course, the lower detection threshold of the *Kepler* observations may very well reveal non-radial modes even in those stars which are considered purely radial pulsators.

One of the main purposes of observing pulsating stars is to compare frequencies in a model of the star with the observed frequencies and to refine the models for best agreement (asteroseismology). For this purpose, mode identification of at least some frequencies is essential. This is most easily done using multicolour photometry (Moya, Garrido & Dupret 2004). An important advantage in studying HADS stars is that one may reasonably assume that the frequencies of highest amplitude are radial modes. This is clearly very important since multicolour data which could be used for mode identification are not available in *Kepler* photometry.

The ratio of first-overtone to fundamental periods, P_1/P_0, for radial modes is a function of P_0. A plot of P_1/P_0 as a function of P_0 is called the Petersen diagram (Petersen 1973). Models show that the period ratio is a unique function of stellar mass and chemical composition for non-rotating stars. One can verify that a pair of modes are indeed radial if the observed period ratio lies on the computed curve in the Petersen diagram, and use the ratio to further refine the stellar parameters, allowing other modes to be identified from the frequencies alone.

Models show that the Petersen diagram is flat for $\log P < -0.9$ (P in d), so that the period ratio is insensitive to mass except for the longer periods. The ratio P_1/P_0 is mostly in the narrow range $0.77 < P_1/P_0 < 0.78$. Lower metallicity has the effect of shifting period ratios towards slightly higher values for the same mass (Poretti et al. 2005). It turns out that a difference in metallicity can balance a difference in mass for $\log P < -0.9$. For longer periods, the position in the Petersen diagram is sensitive to mass. OP and OPAL opacities lead to significantly different period ratios in the Petersen diagram (Lenz et al. 2008), so one needs to be aware of this problem as well.

Even for slow rotators, the effect of rotation on the period ratio can be significant (Suárez, Garrido & Moya 2007). As the star evolves from the main sequence, the frequency of an $l = 2$ mode may approach that of a radial mode through the phenomenon of avoided crossings. When this near-degeneracy in frequency occurs, the oscillation frequency of the radial mode is changed through mode coupling. Coupling can only occur between modes with equal azimuthal orders, m, and spherical degrees, l, differing by 2. When coupling occurs, the radial mode is no longer purely radial. For instance, the character of the fundamental radial mode may remain almost unaltered, but the first overtone may assume a mixed radial/quadrupole character. The effect of near-degeneracy on the frequencies becomes very important for rotational velocities larger than about 15–20 $\mathrm{km\,s^{-1}}$ (Suárez et al. 2007), causing a rapid change in the theoretical period ratio (of the order of 0.01). Neglecting this effect when fitting the observed period ratio would lead to an incorrect determination of metallicity and/or mass.

V2367 Cyg (KIC 9408694) was discovered in a ROTSE survey (Akerlof et al. 2000) and confirmed as a HADS star by Jin et al. (2003) and Pigulski et al. (2009). The star was included in the *Kepler* commissioning run (Quarter 0 = Q0) and data were obtained for a duration of 9.73 d with continuous short-cadence (SC) 1-min exposures. It was not observed in SC mode for the next 409 d, but continuous SC exposures were subsequently obtained for a further 180 d (*Kepler* quarters Q6 and Q7). Fig. 1 shows part of the light curve from SC data. Long-cadence (LC) data (30-min exposures) are also available for Q1, Q2 and Q5. Characteristics of SC data are described in Gilliland et al. (2010), while Jenkins et al. (2010) describe the characteristics of LC data. The light curve has a peak-to-peak amplitude of about 0.4 mag. The maximum brightness level fluctuates by almost 0.1 mag, whereas minimum brightness does not change very much. This star is an excellent candidate for asteroseismology because one may presume that the mode of highest amplitude is a radial mode. Since there is no rotational splitting for radial modes, it provides a very valuable constraint on the models. One would also expect that other radial modes might be present which can be identified from the period ratio in

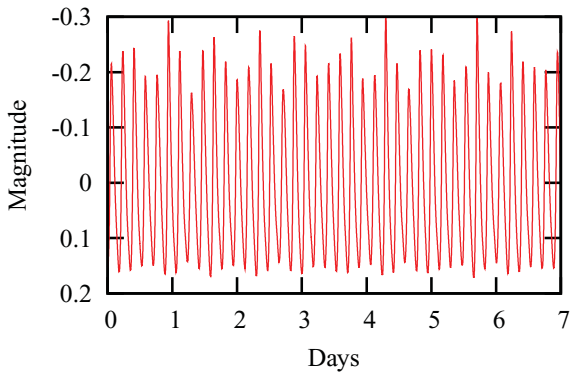

Figure 1. A portion of the light curve of V2367 Cyg from *Kepler* SC data.

© 2011 The Authors, MNRAS **419,** 3028–3038
Monthly Notices of the Royal Astronomical Society © 2011 RAS

Downloaded from http://mnras.oxfordjournals.org/ by guest on March 17, 2016

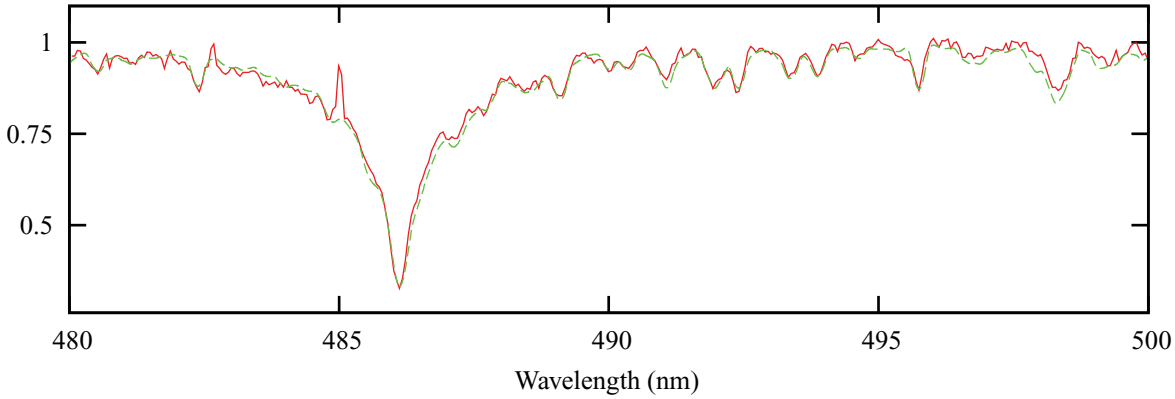

Figure 2. A portion of the spectrum of V2367 Cyg in the region of Hβ (solid line) fitted with a model (dashed line) with $T_{\rm eff} = 7300 \pm 150$ K, $\log g = 3.5 \pm 0.1$ (cgs) and $v \sin i = 100 \pm 10$ km s^{-1}.

the Petersen diagram. In this paper, we present an analysis of the *Kepler* photometry for this star and investigate its potential for asteroseismology.

2 STELLAR PARAMETERS

The KIC lists the following parameters for V2367 Cyg: $T_{\rm eff} = 7500$ K, $R/{\rm R}_\odot = 3.2$, from which $\log L/{\rm L}_\odot = 1.5$. We have used broad-band photometry from TYCHO-2, USNO, TASS, CMC14 and 2MASS to estimate the total observed bolometric flux [$f_{\rm bol} = (7.9 \pm 0.5) \times 10^{-13}$ W m^{-2}]. The infrared flux method (Blackwell & Shallis 1977) was then used with 2MASS magnitudes to determine $T_{\rm eff} = 7280 \pm 180$ K and stellar angular diameter $\theta = 0.029 \pm 0.002$ mas.

We obtained a single spectrum of the star with the Bologna Faint Object Spectrograph & Camera (BFOSC) attached to the 1.5-m Loiano telescope.[1] We used the echelle configuration with Grism #9 and #10 as cross-dispersers. The typical resolution was $R \sim 5000$. The detector was a back-illuminated (EEV) 1300 × 1300 CCD with pixel size 20 μm, readout noise 1.73 e$^-$ and gain 2.1 e$^-$ ADU^{-1}. The spectrum was obtained on the night of 2010 April 22 with exposure time of 2700 s resulting in a signal-to-noise ratio (S/N) ranging from 60 to 100.

Processing of the spectrum involves bias subtraction, flat-field calibration and scattered light correction. Extraction of the spectrum and wavelength calibration was performed using the NOAO/IRAF package.[2]

We determined $T_{\rm eff}$ and $\log g$ of the star by minimizing the difference between the observed and the synthetic Hβ line profiles. For the goodness-of-fit parameter, we used χ^2 defined as

$$\chi^2 = \frac{1}{N} \sum \left(\frac{I_{\rm obs} - I_{\rm th}}{\delta I_{\rm obs}} \right)^2 ,$$

where N is the total number of points, $I_{\rm obs}$ and $I_{\rm th}$ are the intensities of the observed and computed profiles, and $\delta I_{\rm obs}$ is the photon noise. The errors were estimated from the variation in the parameters required to increase χ^2 by 1. As starting values of $T_{\rm eff}$ and $\log g$, we used $T_{\rm eff}$ and $\log g$ derived from the photometry. At the same time, we determined the projected rotational velocity by matching the Mg II λ4481 Å profile with a synthetic profile. The synthetic profiles are computed with SYNTHE (Kurucz & Avrett 1981) on the basis of ATLAS9 (Kurucz 1993) local thermodynamic equilibrium atmosphere models. All models are calculated using the solar opacity distribution function, solar metallicity and a microturbulence velocity of $\xi = 2$ km s^{-1}. The atomic parameters for the spectral lines were taken from Kurucz & Bell (1995).

Fig. 2 shows a comparison between the observed and computed spectra in the Hβ region. The best fit is obtained for $T_{\rm eff} = 7300 \pm 150$ K, $\log g = 3.5 \pm 0.1$ and $v \sin i = 100 \pm 10$ km s^{-1}. The determination of surface gravity was constrained by using the Mg I triplet at 5167–5183 Å, and fixing the magnesium abundance using Mg II λ4481 [log (Mg)/N(tot) = −4.26]. We find that the spectrum is well reproduced by a normal solar abundance. Abundances relative to the solar values (Grevesse et al. 2010) were obtained for the following atomic species: Na [0.1]; Mg [0.1]; Ca [0.0]; Ti [0.4]; Fe [0.1]; Ni [0.0]; and Ba [0.1]. The only anomaly is a very slight overabundance of Ti.

The projected rotational velocity is more than twice that of other HADS stars. From 22 HADS stars with measured $v \sin i$, only three have $v \sin i > 40$ km s^{-1}, the largest value being $v \sin i = 45$ km s^{-1} (Rodríguez et al. 2000). Using the spectroscopic parameters and the calibration of Torres, Andersen & Giménez (2010), we find a luminosity $\log L/{\rm L}_\odot = 1.7 \pm 0.1$, mass $M = 2.2 \pm 0.2$ M$_\odot$, radius $R = 4.5 \pm 0.7$ R$_\odot$ and mean density $\rho = (0.03 \pm 0.01)\rho_\odot$. The location of V2367 Cyg in the theoretical Hertzsprung–Russell (HR) diagram is shown in Fig. 3. In this figure, we use the spectroscopic effective temperature and luminosity. The theoretical red and blue edges for radial overtones shown in the figure are those calculated by Dupret et al. (2004). We note that V2367 Cyg lies within the band occupied by HADS stars and appears to be near the end of core hydrogen burning or just the start of hydrogen shell burning.

In a recent paper on the *Kepler* characterization of the variability among A- and F-type stars (Uytterhoeven et al. 2011), the physical parameters of V2367 Cyg are given as $T_{\rm eff} = 6810 \pm 130$ K, $\log g = 3.80 \pm 0.19$. While the surface gravity is in agreement with ours, the effective temperature is considerably lower than those estimated here from the infrared flux method and our spectrum, which agree very well with each other. Our effective temperature is also very close to the KIC value. Why the effective temperature reported by Uytterhoeven et al. (2011) is so different certainly requires further investigation as it seems well outside the measurement error. A lower effective temperature, if confirmed, will certainly impact the mode identification.

[1] http://www.bo.astro.it/loiano/index.htm

[2] IRAF is distributed by the National Optical Astronomy Observatory, which is operated by the Association of Universities for Research in Astronomy, Inc.

Downloaded from http://mnras.oxfordjournals.org/ by guest on March 17, 2016

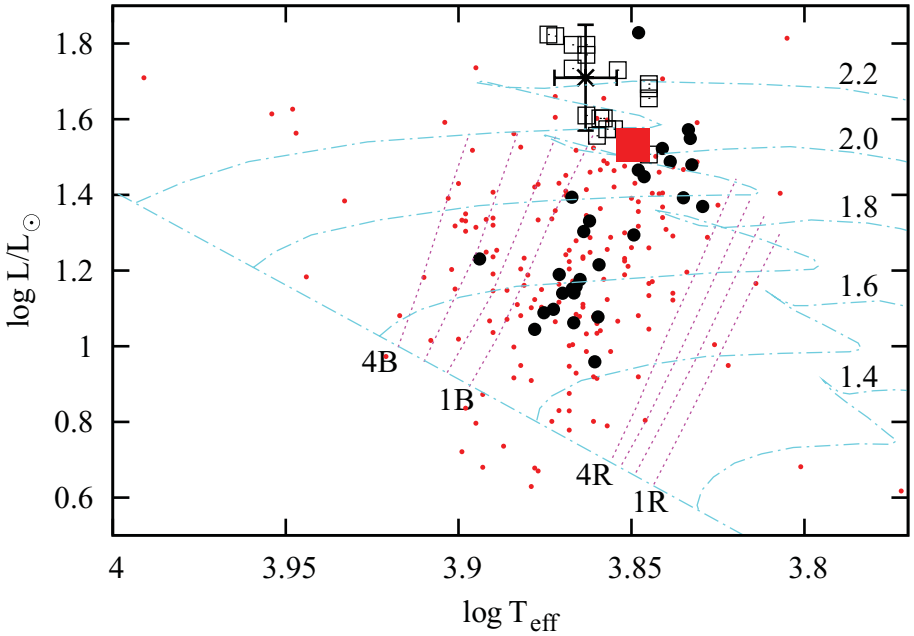

Figure 3. Location of δ Sct stars (small filled circles, derived from Rodríguez et al. 2000), HADS stars (larger filled circles, from McNamara 2000) and V2367 Cyg (cross with 1σ error bars) in the theoretical HR diagram. Pulsation models in Table 2 are shown by the open squares. The best-fitting model which includes mode coupling (Table 4) is shown by the large filled square. Also shown are the zero-age main-sequence, evolutionary tracks for models with masses 1.4–2.2 $M_\odot$ with no core overshoot. The calculated red and blue edges for radial modes p_1, p_2, p_3 and p_4 and mixing length $\alpha = 1.8$ are from Dupret et al. (2004). The fundamental radial red and blue edges are labelled 1R and 1B, while the fourth radial overtone red and blue edges are labelled 4R and 4B.

3 THE *KEPLER* PHOTOMETRY AND FREQUENCY ANALYSIS

V2367 Cyg (KIC 9408694) was observed with continuous 1-min exposures from BJD 245 4953.53 to 245 4963.25 (Run 1: 14 242 observations) and BJD 245 5372.44 to 245 5552.56 (Run 2: 256 767 observations) for a total of 271 009 data points. The 409.2-d gap modifies the usually clean window function. Fig. 4 shows the spectral window in the two runs and in the combined data. Note that the spectral window is about 10 times narrower in Run 2 than in Run 1. This suggests that to extract the frequencies it is probably best to start with Run 2 and to include Run 1 only to refine the frequencies.

Because the amplitudes of the periodic components in this star are so much larger than the noise level, slightly incorrect frequencies will introduce spurious peaks in the periodogram with very high S/N. It is thus imperative to use a technique of non-linear global optimization to determine the frequencies with the greatest possible precision. We started our analysis by performing a periodogram analysis on Run 2 only to extract approximate frequencies for the dominant independent modes, f_1 and f_2. These frequencies were used as starting values in the global optimization technique. This technique consists in fitting frequencies of the form $n_1 f_1 + n_2 f_2$, where n_1 and n_2 are integers with $|n_1| \leq 6$ and $|n_2| \leq 2$. These values of n_1 and n_2 were chosen empirically so as to fit as many of the significant combination peaks as possible without excessive computational demand. The Fourier series was fitted by least squares to the data, and the standard deviation of the residuals, σ, was noted. The two frequencies were systematically changed to search for a global minimum in σ. We found $f_1 = 5.661\,06$ and $f_2 = 7.148\,95\ \mathrm{d}^{-1}$, leading to a residual standard deviation $\sigma = 9.91$ mmag.

Next, we used the value of the third independent frequency, f_3, obtained from the periodogram as a starting value. We fitted a Fourier series of the form $n_1 f_1 + n_3 f_3$ which led to a global minimum when $f_3 = 7.775\,64\ \mathrm{d}^{-1}$ and $\sigma = 15.00$ mmag. Using these optimum values of f_1, f_2 and f_3 as starting values, we fitted a Fourier series, with frequencies of the form $n_1 f_1 + n_2 f_2 + n_3 f_3$ and $|n_1| \leq 6$, $|n_2| \leq 2$ and $|n_3| \leq 1$, to the Run 2 data. The optimum solution is $f_1 = 5.661\,06$, $f_2 = 7.148\,95$ and $f_3 = 7.775\,65\ \mathrm{d}^{-1}$ leading to a residual standard deviation of $\sigma = 4.21$ mmag. Finally, we took

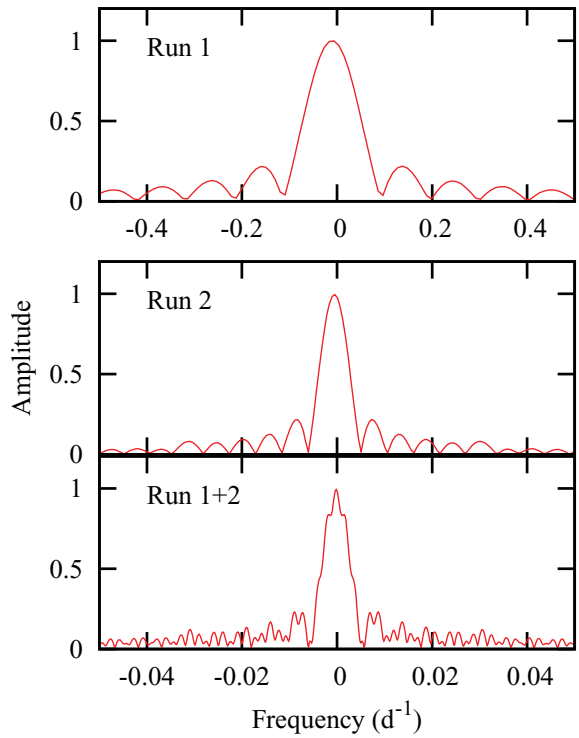

Figure 4. The spectral window in the first, second and combined runs of the *Kepler* data.

© 2011 The Authors, MNRAS **419,** 3028–3038
Monthly Notices of the Royal Astronomical Society © 2011 RAS

Downloaded from http://mnras.oxfordjournals.org/ by guest on March 17, 2016

Table 1. Frequencies, f_n (d^{-1}), amplitudes, A (mmag), and phases, ϕ (rad), for the most certain independent frequencies from the least-squares solution of the combined data. The epoch of phase zero is BJD 245 4950.00.

n	f_n (d^{-1})	A (mmag)	ϕ (rad)
1	5.661 058 ± 0.000 003	155.537 ± 0.005	2.006 13 ± 0.000 03
2	7.148 949 ± 0.000 029	16.833 ± 0.004	−0.216 42 ± 0.000 26
3	7.775 566 ± 0.000 054	8.935 ± 0.004	−0.090 11 ± 0.000 50
4	10.122 470 ± 0.000 043	2.481 ± 0.004	2.695 20 ± 0.001 81
5	9.815 725 ± 0.000 229	1.959 ± 0.004	1.729 36 ± 0.002 31
6	7.853 158 ± 0.000 325	1.506 ± 0.004	−2.249 30 ± 0.002 98
7	2.956 421 ± 0.000 400	1.296 ± 0.004	−1.671 54 ± 0.003 48
8	10.023 980 ± 0.000 440	1.113 ± 0.004	−1.581 70 ± 0.004 04
9	7.683 311 ± 0.000 427	1.067 ± 0.004	−1.714 67 ± 0.004 21
10	19.391 180 ± 0.000 631	0.733 ± 0.004	−2.724 27 ± 0.006 14
11	22.108 459 ± 0.000 668	0.653 ± 0.004	−2.321 21 ± 0.006 95
12	16.389 999 ± 0.000 804	0.541 ± 0.004	−1.005 80 ± 0.008 33
13	16.447 281 ± 0.000 900	0.518 ± 0.004	2.894 42 ± 0.008 73
14	16.543 739 ± 0.000 969	0.496 ± 0.004	−0.512 26 ± 0.009 10
15	16.487 141 ± 0.001 150	0.398 ± 0.004	0.831 12 ± 0.011 32

these values of f_1, f_2 and f_3 as starting values for an optimal solution to the combined data (Run 1 + Run 2). For the same values of n_1, n_2 and n_3, we find very nearly the same solution as for Run 2: $f_1 = 5.661\,058(\pm3)$, $f_2 = 7.148\,949(\pm29)$ and $f_3 = 7.775\,566(\pm54)$ d^{-1}, giving $\sigma = 4.21$ mmag.

To facilitate extraction of further independent frequencies, we fitted a Fourier series involving f_1, f_2 and f_3 with $|n_1| \leq 8$, $|n_2| \leq 2|$ and $|n_3| \leq 1$ (127 frequencies) and removed them from the data. We calculated the periodogram and extracted over 500 significant additional frequencies. The level of significance was judged by the commonly used four sigma rule: a peak is significant if its amplitude is at least four times higher than the background noise level in the periodogram (Breger et al. 1993). There is still some residual power in the form of a close doublet at f_1. This is probably a result of amplitude variability (see below). As more and more lower amplitude frequencies are considered, it becomes easier to match them with combinations of higher amplitude frequencies and it is no longer possible to determine whether they are truly independent. In Table 1, we list those frequencies which are almost certainly independent. These frequencies have amplitudes that are too high to allow an interpretation as combination frequencies. The periodogram after removal of f_1, f_2 and f_3 and their combinations is shown in Fig. 5.

The low-frequency mode $f_7 = 2.956\,42$ d^{-1} is particularly interesting. Low frequencies driven by the convective blocking mechanism are thought to be responsible for pulsations in the γ Doradus (γ Dor) stars (Guzik et al. 2000). The effective temperature of V2367 Cyg is slightly too high for convective blocking to work, but considering the error in $T_{\rm eff}$ one can certainly not rule out the possibility that this star is a δ Sct–γ Dor hybrid. Assuming $M = 2.2\,M_\odot$, $R = 4.5\,R_\odot$ and the observed $v \sin i = 100$ km s^{-1}, the minimum rotational frequency is 0.44 d^{-1} and the critical rotational frequency is 1.28 d^{-1}. The critical equatorial rotational velocity is about 300 km s^{-1}, implying an inclination $i = 20°$ if the star is rotating at this velocity. It thus appears that f_7 cannot be the rotational frequency.

The amplitude variation of the dominant frequencies was investigated. First, a global solution, which included approximately 70 terms for LC and SC data, was obtained using non-linear least squares. For each independent frequency, separate residuals were calculated: they included only a given frequency and its harmonics with all the other terms subtracted. Using these residuals, overlapping 20-d subsets were created, with the starting epoch shifted by 2 d. For Q0, a single subset was created. Data from different quarters were kept separate. A single frequency was then fitted to all subsets. The resulting amplitudes are plotted in Fig. 6.

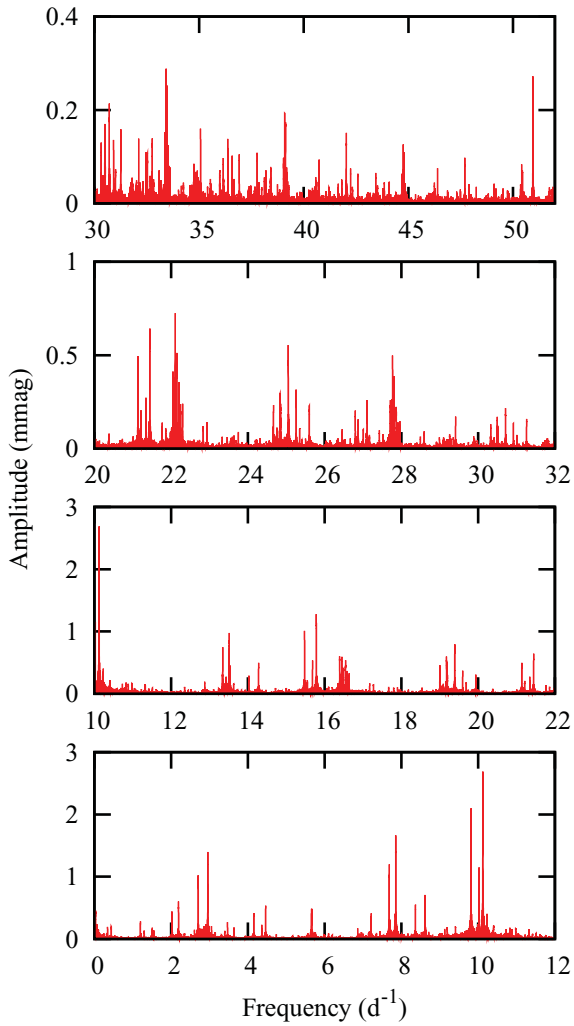

Figure 5. Periodogram after removal of f_1, f_2, f_3 and their combination frequencies.

For f_1, there is a jump in amplitude of about 0.7 per cent between Q6 and Q7. The same jump is seen for the harmonics $2f_1$ and $3f_1$. The jump is probably a result of a change in detector, which occurs as the field is rotated between quarters. Since the same detector is used for a given field every four quarters, data for Q0+Q1 and Q5 can be directly compared and so can data for Q2 and Q6 or for Q3 and Q7. Unfortunately, data for Q3 and Q4 are not available for V2367 Cyg. The behaviour of f_1 and its two harmonics is similar, which means that the shape of light curve for this mode does not change. The small changes in amplitude for f_1 within a given quarter, which are less than 0.3 per cent, may be real.

Because of the longer exposure time in LC data, there is an averaging effect and the amplitudes are correspondingly lower than in SC data. The effect depends on frequency: the higher the frequency, the greater the reduction in amplitude. This effect is clearly visible for $3f_1$ where the reduction in amplitude for LC data is greatest at about 20 per cent. For f_2 and f_3, the amplitude jump between Q6

Downloaded from http://mnras.oxfordjournals.org/ by guest on March 17, 2016

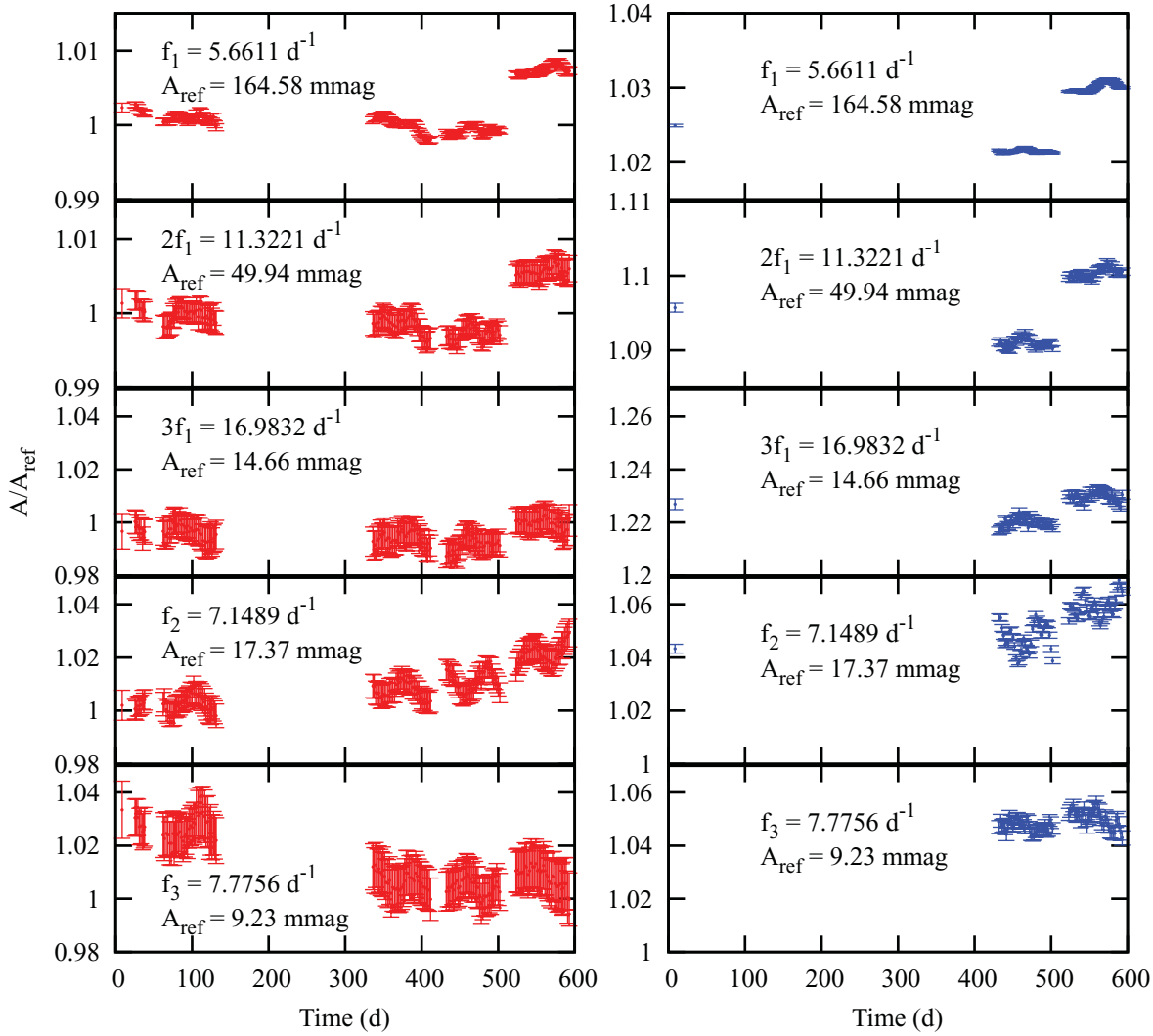

Figure 6. Relative amplitude variation for the three principal independent modes and two harmonics of f_1 as a function of time. The ratio of the amplitude relative to the reference amplitude, $A_{\rm ref}$, is plotted as a function of time. The left-hand panels are from LC data and the right-hand panels are from SC data. Note the higher amplitude ratio for SC data.

and Q7 is not very clear, but is in fact about the same (0.7 per cent) as for f_1 and its harmonics.

In conclusion, there does seem to be evidence of changes in amplitude of the principal modes during the course of the observations, but the result must remain uncertain because external factors (change in detector, ageing of the detector) play an important role. The small-scale amplitude changes are perhaps more secure and deserve further investigation.

4 COMBINATION FREQUENCIES

Several different non-linear mechanisms may be responsible for generating combination frequencies between two independent frequencies, ν_1 and ν_2. For example, any non-linear transformation, such as the dependence of emergent flux variation on the temperature variation ($F = \sigma T^4$) will lead to cross-terms involving frequencies $\nu_1 + \nu_2$ and $\nu_1 - \nu_2$ and other combinations. The inability of the stellar medium to respond linearly to the pulsational wave is another example of this effect. Combination frequencies may also arise through resonant mode coupling when ν_1 and ν_2 are related in a simple numerical way, such as $2\nu_1 \approx 3\nu_2$.

The interest in the combination frequencies derives from the fact that their amplitudes and phases may allow indirect mode identification. For non-radial modes, some combination frequencies are not allowed depending on the parity of the modes (Buchler, Goupil & Hansen 1997) which could lead to useful constraints on mode identification. Combination frequencies also arise through non-linear interaction of two modes. Suppose a mode with frequency ν_1, phase ϕ_1, interacts with a mode of frequency ν_2, phase ϕ_2. To first order, the interaction terms will be the product of the two eigenfunctions integrated over the star, leading to a frequency $\nu_2 - \nu_1$ with phase $\phi_2 - \phi_1$ and frequency $\nu_2 + \nu_1$ with phase $\phi_2 + \phi_1$.

Suppose that we have two modes with frequencies $n_1\nu_1$ and $n_2\nu_2$ (harmonics of frequencies ν_1 and ν_2) and that we measure phase $\phi_{\rm c}$ for the combination frequency $n_1\nu_1 + n_2\nu_2$. Since, to first order, the phase of the combination frequency will be $n_1\phi_1 + n_2\phi_2$, then $\phi_{\rm r} = \phi_{\rm c} - (n_1\phi_1 + n_2\phi_2)$ can be expected to be zero at some level of approximation (Buchler et al. 1997; Degroote et al. 2009). In the β Cep star HD 180642 observed by *CoRoT*, Degroote et al. (2009)

Downloaded from http://mnras.oxfordjournals.org/ by guest on March 17, 2016

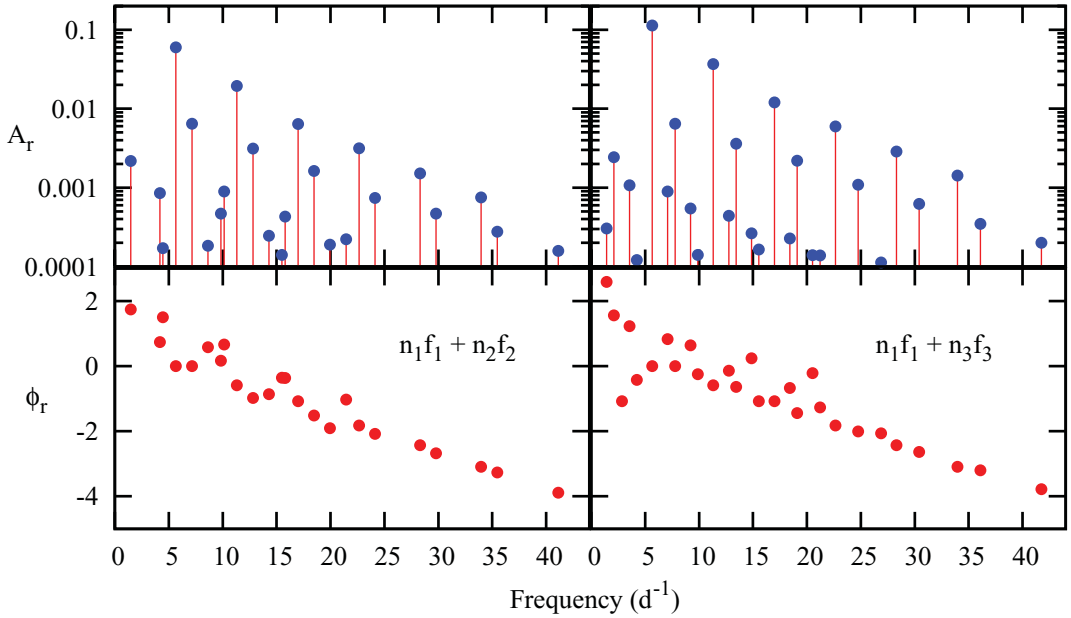

Figure 7. The relative amplitude, $A_r = A_c/(A_iA_j)$, which is the ratio of the combination frequency amplitude, A_c, to the product of the parent frequency amplitudes A_i, A_j, is shown as a function of frequency in the top panels. In calculating A_r, amplitudes are measured in mmag. The relative phase, $\phi_r = \phi_c - (n_i\phi_i + n_j\phi_j)$, which is a function of the phase of the combination frequency, ϕ_c, and the phases, ϕ_i, ϕ_j of the parent frequencies, is shown in the bottom panels. Combination frequencies involving f_1 and f_2 are shown in the left-hand panels and those involving f_1 and f_3 in the right-hand panels.

finds that ϕ_r varies from mode to mode: there is no correlation of ϕ_r with frequency. In the δ Sct star KIC 9700322, on the other hand, there is a strong correlation of ϕ_r with frequency (Breger et al. 2011). The amplitude, A_c, of a combination frequency relative to the product of the amplitudes of the parent frequencies, A_iA_j, is also interesting. The ratio $A_r = A_c/(A_iA_j)$ is typically around 0.003 (when measured in mmag) in the δ Sct stars 44 Tau (Breger & Lenz 2008) and KIC 9700322 (Breger et al. 2011). In Fig. 7, we show A_c as a function of frequency for combination modes involving f_1, f_2 and f_1, f_3.

We investigated the behaviour of ϕ_r and A_r for the combination frequencies involving f_1 and f_2. There is a very clear relationship between ϕ_r and frequency (Fig. 7, left-hand panels). The relationship is well represented by $\phi_r = 1.389 - 0.1352f$ with ϕ_r in rad and f in d^{-1}. Almost the same relationship is exhibited by combination frequencies involving f_1 and f_3 (Fig. 7, right-hand panels). Several other δ Sct stars were investigated and in all of them a distinct correlation is found between ϕ_r and frequency with $\partial\phi_r/\partial f \approx -0.1$.

This intriguing relationship demands an explanation. Phase differences between various photometric bands in δ Sct stars arise due to a combination of geometric and temperature effects, which makes these differences useful in mode identification. One of the important parameters that contributes to this effect is the ratio of flux variation to displacement which occurs in the photosphere during pulsation. This ratio, usually called f, is complex in pulsation models of δ Sct stars and introduces a phase difference in the light variation. It turns out that both the real and the imaginary parts of f strongly depend on frequency and are only weakly dependent on the spherical harmonic degree. One may expect that this may at least be partly responsible for the strong correlation between ϕ_r and frequency, but further investigations are required.

We also note that there are clear logarithmic variations of A_r with frequency which are different for different mode combinations. The family involving n_1f_1 has the highest values of A_c which is well represented by $A_c = -0.948 - 0.0663\log_{10}f$. The next most dominant family involves combinations of the form $n_1f_1 + f_2$ and can be represented by $A_c = -1.904 - 0.0472\log_{10}f$.

5 MODELLING

In order to model the oscillations in V2367 Cyg, we need to identify the modes. This is not an easy task for δ Sct stars, even when multicolour photometry and/or high-dispersion line profile observations are available (see e.g. Casas et al. 2006; Poretti et al. 2009). Rotation is a major problem in this regard because it modifies the stellar structure and the physical processes occurring in the stellar interior. This causes additional uncertainties in the interpretation of the oscillation spectra, and greatly affects the oscillation spectrum (see Goupil et al. 2005, for a review on this topic).

Recent studies (Lignières, Rieutord & Reese 2006; Reese, Lignières & Rieutord 2008) using a non-perturbative approach lead to a different distribution of the oscillation modes in rapidly rotating stars. Recently, Reese et al. (2009b) have proposed a semi-empirical method for identifying modes in rapidly rotating stars. Non-perturbative calculations based on polytropic models converge to those obtained with classical perturbation methods only when the rotational frequency is much smaller than the pulsational frequency.

V2367 Cyg has a relatively large projected rotational velocity ($v \sin i = 100\,\mathrm{km\,s^{-1}}$) and the deformation is significant, so that perturbation techniques are likely to fail, the failure coming first for high-order modes. In this work, we use a perturbation method to calculate the frequencies under the following considerations: (1) since V2367 Cyg is a HADS star, it is reasonable to expect that radial modes will be excited along with non-radial modes; (2) in Suárez, Bruntt & Buzasi (2005), the authors show that second-order perturbation calculations, which include second-order near-degeneracy, result in a linear dependence of the radial-mode period ratios with rotational frequency for rotational velocities up to about

Downloaded from http://mnras.oxfordjournals.org/ by guest on March 17, 2016

$100\,\mathrm{km\,s^{-1}}$; and (3) although non-perturbative calculations have recently been applied to models more sophisticated than polytropes (Reese et al. 2009a), they have not yet been done with realistic stellar models.

5.1 Mode identification: radial modes

The above considerations clearly imply that no satisfactory solution can be expected, given the current level of modelling in the presence of rotation. Nevertheless, some progress might be possible by careful consideration of all available data.

In a HADS star, it is a reasonable first step to suppose that the mode of highest amplitude is a radial mode (not necessarily the fundamental radial mode). If we tentatively assume that f_1 is the fundamental radial mode, one should be able to roughly estimate the mean density of the star, $\bar{\rho}$, using the simple relationship $P\sqrt{\bar{\rho}/\bar{\rho}_\odot} = Q$. Assuming $Q = 0.033\,\mathrm{d}$ for a typical radial pulsator gives $\bar{\rho}/\bar{\rho}_\odot = 0.035$. The mass and radius of V2367 Cyg determined using Torres et al. (2010) give a stellar density of $\rho/\bar{\rho}_\odot = 0.025 \pm 0.012$ which is consistent with this value. This argument at least suggests that a radial mode at this frequency is consistent with what little information we have of the star.

If f_1 is the fundamental radial mode, we may hope to locate the first-overtone radial mode because we know from models that the period ratio of the first-overtone to fundamental radial mode is in the range $0.77 < P_1/P_0 < 0.78$. The observed period ratios which involve f_1 and four other independent modes of highest amplitude are as follows: $f_1/f_2 = 0.792$, $f_1/f_3 = 0.728$, $f_1/f_6 = 0.721$, $f_1/f_9 = 0.737$. None of these ratios falls within the range mentioned above. Our argument has been that the radial modes should be of high amplitude, but the modes which roughly fit the expected period ratio have such low amplitude as to destroy the credibility of this argument.

Our next step is to examine models in more detail to see if any comes close to meeting our assumptions by relaxing the condition that f_1 should be the fundamental radial mode. We start by assuming that the two modes of largest amplitude, f_1 and f_2, are both radial. Table 2 summarizes the results of this survey. All models were calculated assuming no rotation.

The linear non-adiabatic models developed by MM are based on the hydrodynamical code originally developed in Los Alamaos (see e.g. Stellingwerf 1982; Bono & Stellingwerf 1994) and subsequently adapted to pre-main-sequence δ Sct stars (Marconi & Palla 1998). The CESAM code (Morel & Lebreton 2008) and the GRACO code (Moya et al. 2004) were used by AM. AG computed stellar equilibrium models using CLES (Scuflaire et al. 2008b) and the non-adiabatic non-radial code MAD (Dupret 2001) which includes a time-dependent convection treatment described in Grigahcène et al. (2005). The models were specifically chosen so that the radial modes are unstable. MDiC used the ATON code for stellar evolution (Ventura et al. 1998) in the standard version for asteroseismic applications (D'Antona et al. 2005). The LOSC adiabatic oscillation code by Scuflaire et al. (2008a) was used to calculate the frequencies of radial modes. JD-D used the Warsaw–New Jersey evolutionary code by Paczynski and the non-adiabatic pulsation code by Dziembowski (1977).

In Table 2, we not only considered f_1 and f_2 as possible radial modes, but also took into account the possibility that f_1 may be the first harmonic. Since the expected frequency ratio of fundamental to first overtone is about 0.775, we expect the fundamental frequency to be about $4.36\,\mathrm{d^{-1}}$. The nearest observed frequency to this value is a low-amplitude mode at $f_{69} = 4.3655\,\mathrm{d^{-1}}$ (amplitude 0.2 mmag), which, for the purposes of the exercise, we could assume to be the fundamental radial mode when f_1 is taken as the first overtone. We now suppose that f_2 is the second overtone so that we have $f_{69}/f_1 = P_1/P_0 = 0.771$ and $f_1/f_2 = P_1/P_2 = 0.792$. We see from Table 2 that there are models for which P_1/P_0 is in good agreement with observations. Unfortunately, in these models, there is poor agreement between the observed and calculated frequencies. We show the agreement between observations and models in Fig. 8.

The models of Table 2 are shown in Fig. 3 as the open squares. We see from this figure that most of the models are within the general error box. The main difficulty with the models, however, is

Table 2. Survey of some non-rotating models which attempt to match $f_1 = 5.6611$ and $f_2 = 7.1490\,\mathrm{d^{-1}}$ by radial modes. The columns labelled ν_0, ν_1 and ν_2 are the frequencies of fundamental, first- and second-overtone radial modes (in $\mathrm{d^{-1}}$). Frequencies in brackets indicate stable modes. The models by MDiC are adiabatic and therefore provide no information about the stability of the modes. The ratios of first-overtone to fundamental periods, P_1/P_0, and second-overtone to first-overtone periods, P_2/P_1, are given where appropriate.

N	Author	$M/\mathrm{M}_\odot$	$\log T_{\mathrm{eff}}$	$\log L/\mathrm{L}_\odot$	ν_0	ν_1	ν_2	P_1/P_0	P_2/P_1
1	MM	2.0	3.860	1.556	(7.370)	(9.249)	(11.158)	–	–
2	AM	2.1	3.857	1.574	5.55	7.22	9.05	0.769	–
3	AG	2.2	3.855	1.574	5.621	7.286	9.120	0.771	–
4	MM	2.2	3.863	1.61	(5.661)	(7.342)	(9.205)	0.771	–
5	MM	2.25	3.854	1.73	(4.340)	(5.661)	(7.111)	0.767	0.796
6	MM	2.3	3.863	1.77	(4.344)	(5.660)	(7.110)	0.767	0.796
7	MDiC	2.3	3.859	1.602	5.71	7.36	9.18	0.776	0.802
8	MDiC	2.3	3.858	1.602	5.65	7.28	9.08	0.776	0.802
9	MDiC	2.3	3.867	1.734	4.81	6.21	7.76	0.774	0.800
10	MDiC	2.3	3.863	1.797	4.46	5.76	7.19	0.774	0.801
11	MM	2.4	3.872	1.82	(4.354)	(5.661)	(7.111)	0.769	0.796
12	MDiC	2.5	3.867	1.797	4.35	5.62	7.01	0.774	0.802
13	JD-D	2.5	3.874	1.824	(4.370)	(5.661)	(7.098)	0.772	0.798
14	MM	2.0	3.845	1.507	–	(5.655)	(7.361)	–	0.768
15	MM	2.0	3.845	1.655	(4.331)	(5.678)	(7.142)	0.763	0.795
16	MM	2.2	3.845	1.682	(4.351)	(5.682)	(7.133)	0.766	0.796
17	MM	2.3	3.845	1.693	(4.372)	(5.693)	(7.150)	0.768	0.797

Downloaded from http://mnras.oxfordjournals.org/ by guest on March 17, 2016

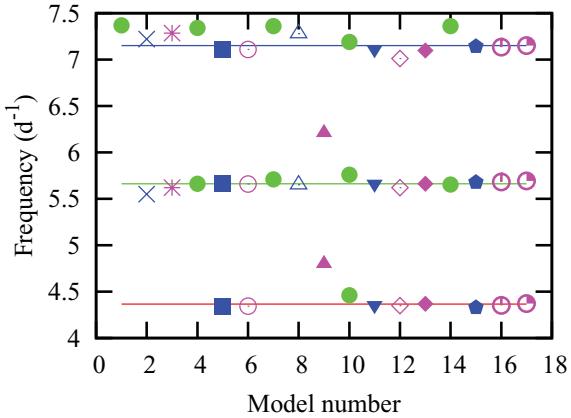

Figure 8. Comparison of observed frequencies (lines) with model frequencies (points). The different symbols are used to guide the eye to frequencies belonging to the same model.

that in most cases the radial modes are stable. This is not surprising because they are all close to the blue edge of the instability strip.

Because of these problems, it is interesting to investigate models in which we relax the condition that either f_1 or f_2 is a radial mode. Some non-rotating models of this nature are shown in Table 3. These models, computed by DP and MS, used evolutionary models from the CESAM2K code (Morel 1997). The model eigenspectra were computed using the LNAWENR linear, non-radial, non-adiabatic stellar pulsation code (Suran 2008). Although the models provide a very good fit to the observed frequencies, we are still faced with the problem that all radial modes are stable. The additional problem when allowing non-radial modes is that rotation has a much larger effect on their frequencies than for radial modes. A full solution which includes rotation is required before the frequencies of non-radial modes can be compared with observations.

This exercise tells us that it is possible to fit the two frequencies of highest amplitude with the first and second radial overtones with a maximum uncertainty of only 0.5 per cent. It is even easier to relax the condition that one of the modes be radial, but this is a dead-end approach because we do not know the rotational profile and one cannot use non-rotating models for this purpose. The main problem in all cases, however, is that the radial modes are stable because the star is too close to the blue edge.

5.2 Near-degeneracy effects on period ratios

The role of mode coupling (near-degeneracy) on radial period ratios has been extensively discussed by Suárez et al. (2005), Suárez, Garrido & Goupil (2006) and Suárez et al. (2007). They explored the theoretical effects of rotation in calculating the period ratios of double-mode radial pulsating stars with special emphasis on HADS stars. In Suárez et al. (2006), the effect of moderate rotation on both evolutionary models and oscillation frequencies is considered. They show that these effects are important and should not be neglected, as we have done. In particular, differences in period ratios of some hundredths can be obtained even for low-to-moderate rotational velocities (15–50 km s^{-1}). In Suárez et al. (2007), an analysis of the relative intrinsic amplitudes of near-degenerate modes shows that the identity of the fundamental radial mode and the rotationally coupled quadrupole mode remains almost unaltered once near-degeneracy effects are considered. The situation is different for the first overtone which has a mixed character. The effect of near-degeneracy on the oscillation frequencies becomes very important for rotational velocities larger than about 15–20 km s^{-1}, and the period ratio is severely affected. This, in turn, leads to an uncertainty in using the Petersen diagram to estimate the metallicity. This also leads to ambiguities in mass determination of as much as 0.5 M$_\odot$.

In the case of V2367 Cyg with $v \sin i = 100$ km s^{-1}, the above studies indicate quite clearly the need to take rotational coupling into account. The important fact here is that if a radial mode and a $(l, m) = (2, 0)$ mode are close enough, then they will repel each other. We can try to use this effect to reproduce the period ratio observed in V2367 Cyg. We assume that f_1 is the radial fundamental mode and check whether f_2 or f_3 can be reproduced as a radial mode. This means we have to find a model with $l = 2$ modes such that the frequencies of radial modes are modified for better agreement with observations. We also assume that rotational coupling mostly affects f_2 or f_3 while leaving f_1 relatively unaffected.

If a radial mode is affected by rotational coupling with a quadrupole mode, their relative amplitudes will be modified due to mode mixing, since the mode is no longer purely radial (Daszyńska-Daszkiewicz et al. 2002). Since f_2 and f_3 have much lower amplitudes than f_1, it is reasonable to assume that mode coupling has affected one or both of these modes rather than the f_1 mode. In addition to rotation, convective core overshooting is an important factor in the investigation because it changes the frequencies of $l = 2$ modes.

We examined models with different chemical composition and also varied other parameters. In principle, a high period ratio $P_1/P_0 = 0.792$ can be attained by reducing the metallicity significantly and increasing the helium abundance, but these changes move the corresponding models rather far from the observed values in the HR diagram. Moreover, there are no indications of low metallicity from the admittedly poor-S/N spectra that we obtained. Our codes use the formalisms described in Soufi, Goupil & Dziembowski (1998) and Dziembowski (1977). These codes have been used, for example, in Daszyńska-Daszkiewicz et al. (2002).

After several trials, we eventually found a model that fits f_1 and f_2, as radial modes. In this model, f_1 is the fundamental radial mode and f_2 the first overtone. Furthermore, both modes are unstable. In our model, f_3 could be an axisymmetric dipole mode (frequency 7.82 d^{-1}, observed frequency 7.77 d^{-1}), but this might

Table 3. Models in which non-radial modes are included. The value of l is shown in brackets. A plus sign means the mode is driven and a minus sign means that it is damped. The last column is the χ^2 value of the fit to observed frequencies (frequencies are in d^{-1}).

N	Author	M/M$_\odot$	log $T_{\rm eff}$	log L/L$_\odot$	f_1	f_2	f_3	f_6	χ^2
1	DP/MS	2.24	3.873	1.71	5.661(+2)	7.150(−0)	7.774(+1)	7.860(+3)	2.1564
2		2.10	3.855	1.61	5.661(−0)	7.150(+2)	7.774(+3)	7.860(+3)	2.1653
3		2.26	3.856	1.73	5.661(+2)	7.150(+3)	7.774(+3)	7.860(+1)	1.3883
4		2.26	3.856	1.73	5.661(−0)	7.150(+3)	7.774(+3)	7.860(+1)	1.4636

Downloaded from http://mnras.oxfordjournals.org/ by guest on March 17, 2016

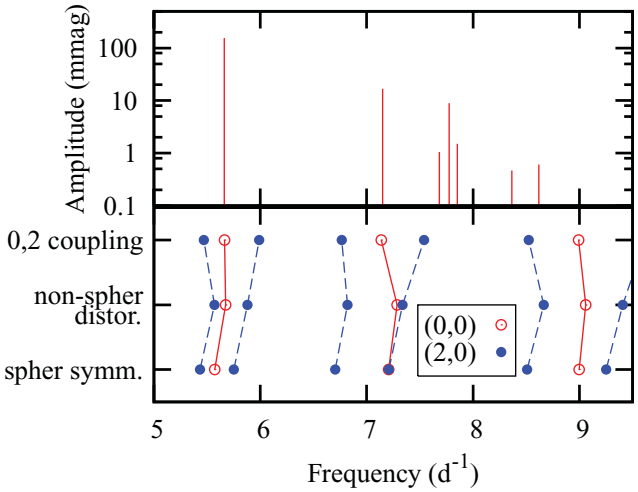

Figure 9. Lower panel: changes in model frequencies of $(l, m) = (0, 0)$ and (2, 0) modes due to different effects. 'spher symm' includes effects of the horizontally averaged centrifugal force in the equilibrium model. In 'non-spher distor', frequencies are determined from the perturbation method, taking into account non-spherically symmetric distortion due to the centrifugal force and second- and third-order Coriolis effects. In '0,2 coupling', the rotational coupling effect between radial and nearby quadrupole modes is added. The red solid lines and open circles refer to radial modes and the blue dashed lines and filled circles to quadrupole modes as indicated in the box. Top panel: schematic diagram of the observed independent frequencies.

be an accidental agreement. In Fig. 9, we show how radial modes and quadrupole modes interact with each other, and the effects of distortion of spherical symmetry and mode coupling in the model. Unfortunately, the other observed frequencies do not match the model frequencies very well. The model is in the secondary contraction phase. We searched for a suitable frequency match in models in the main-sequence and post-main-sequence phases, but failed to find any that met the required conditions.

Concerning the validity of the perturbation approach that we have used, it may be useful to note that in this model $\Omega/\omega = 0.11$ for f_1, where Ω is the angular frequency of rotation, and ω is the angular frequency of the mode. While a non-perturbative approach would be better, we feel that Ω/ω is sufficiently small and that the perturbation technique is not unreasonable in this case.

We conclude that it is not impossible to match the two dominant modes in this star as radial modes, but only if rotational coupling is taken into account. Note that at the fairly high rotational rate in this star, the perturbation method that we used may not be very accurate. The model just described places the star in the secondary gravitational contraction phase. The model is shown as the filled red square in Fig. 3 and listed in Table 4. The effective temperature and luminosity of the model is close to the spectroscopically measured value. Although this model fails to fit other frequencies, it provides a good starting solution for a more detailed investigation.

Table 4. Parameters for a model which includes rotational mode coupling.

Author	$M/\mathrm{M}_\odot$	$\log T_{\mathrm{eff}}$	$\log L/\mathrm{L}_\odot$	f_1	f_2
Observed	–	–	–	5.661	7.149
PL	2.10	3.8497	1.531	5.663	7.138

It is also encouraging to note that f_1 is matched by the fundamental radial mode rather than the first overtone. A match of f_1 to the first overtone means that the star has a lower density and larger radius, making it more luminous and therefore a less satisfactory match to observations. It also fits the perception that a mode with such an overwhelmingly larger amplitude should be radial.

6 CONCLUSIONS

Although the principal modes in HADS stars are generally considered to be radial, the period ratios in V2367 Cyg do not match the ratios of radial modes in models which do not include rotation or mode coupling. Moreover, in those models where the ratio is closest to the observed ratio, the modes are usually stable. Because the projected rotational velocity of V2367 Cyg is the highest of the HADS stars, models neglecting rotation and mode coupling are not appropriate in studying this star.

Even moderate rotation can have a significant effect on the radial-mode period ratios through coupling with a nearby quadrupole mode (Suárez et al. 2006, 2007). Using a perturbation method, we were able to match the two principal frequencies, f_1 and f_2, in V2367 Cyg with fundamental and first-overtone radial modes by choosing the conditions where a nearby $l = 2$ mode could affect the frequency f_2 to the required extent. The resulting model with solar abundance places the star in the secondary gravitational contraction phase with mass $M/\mathrm{M}_\odot = 2.10$, $\log T_{\mathrm{eff}} = 3.8497$ and $\log L/\mathrm{L}_\odot = 1.531$. The calculated period ratio is in good agreement with observations. Both modes are unstable in the model and the location of the model in the HR diagram is close to the observed location derived from the spectrum of the star. Unfortunately, other frequencies do not produce a good match. Therefore, we do not believe that this model correctly describes the star. There may be other possible models that fit in other evolutionary stages. Moreover, we have to keep in mind that the use of a perturbation approach may not be entirely valid at the relatively high rotation of this star. It would be important to use a non-perturbative approach for such a rapid rotator. This study is outside the scope of this work, but the model presented here might be used as a good starting point.

In a HADS star observed by *CoRoT*, Poretti et al. (2011) find that there is evidence for a small amplitude modulation of the principal mode. In V2367 Cyg, we found amplitude modulation, but this can be largely explained as an instrumental effect.

Unexplained low frequencies are present in most δ Sct stars (Grigahcène et al. 2010) and in non-pulsating A-type stars in general (Balona 2011). V2367 Cyg is no exception: there is at least one low frequency ($f_7 = 2.956\,42\,\mathrm{d}^{-1}$) which is outside the frequency domain of δ Sct stars and cannot be explained by rotation. The star could be considered a δ Sct–γ Dor hybrid, but this must remain speculative until the nature of these low frequencies is understood.

The expected and observed phase differences of combination modes correlate with the frequencies of these modes. We investigated some other δ Sct stars (HADS stars and otherwise) and find a similar relationship. This correlation is not understood and the problem requires further investigation.

There is no doubt that ground-based multicolour photometry is an important requirement for further progress in modelling V2367 Cyg. This will be an essential requirement to verify that f_1 and f_2 are both radial and, hopefully, to identify a few more modes. It is certainly necessary to take into account the high rotational velocity of the star. While this is a complicating factor, it does test the limits of our current modelling capabilities. The extremely

Downloaded from http://mnras.oxfordjournals.org/ by guest on March 17, 2016

high precision of *Kepler* photometry is a huge advantage in this respect.

ACKNOWLEDGMENTS

The authors wish to thank the *Kepler* team for their generosity in allowing the data to be released to the Kepler Asteroseismic Science Consortium ahead of public release and for their outstanding efforts which have made these results possible. Funding for the *Kepler* mission is provided by NASA's Science Mission Directorate.

LAB wishes to thank the South African Astronomical Observatory for financial support. PL acknowledges partial financial support from the Polish MNiSW grant N N203 379 636; AP acknowledges the Polish MNiSzW grant N N203 302635 and JM-Ż acknowledges the Polish grant N N203 405139. VA and GH were supported by the Austrian Fonds zur Förderung der wissenschaftlichen Forschung under grant P20526-N16. AM acknowledges the funding of Astro-Madrid (CAMS2009/ESP-1496) and the Spanish grants ESP2007-65475-C02-02, AYA 2010-21161-C02-02 and CSD2006-00070.

We thank Ennio Poretti for useful discussions.

REFERENCES

Akerlof C. et al., 2000, AJ, 119, 1901
Balona L. A., 2011, MNRAS, 415, 1691
Blackwell D. E., Shallis M. J., 1977, MNRAS, 180, 177
Bono G., Stellingwerf R. F., 1994, ApJS, 93, 233
Breger M., 2007, Commun. Asteroseismol., 150, 25
Breger M., Lenz P., 2008, A&A, 488, 643
Breger M. et al., 1993, A&A, 271, 482
Breger M. et al., 2011, MNRAS, 414, 1721
Brown T. M., Latham D. W., Everett M. E., Esquerdo G. A., 2011, AJ, 142, 112
Buchler J. R., Goupil M., Hansen C. J., 1997, A&A, 321, 159
Casas R., Suárez J. C., Moya A., Garrido R., 2006, A&A, 455, 1019
D'Antona F., Cardini D., Di Mauro M. P., Maceroni C., Mazzitelli I., Montalbán J., 2005, MNRAS, 363, 847
Daszyńska-Daszkiewicz J., Dziembowski W. A., Pamyatnykh A. A., Goupil M., 2002, A&A, 392, 151
Degroote P. et al., 2009, A&A, 506, 111
Derekas A. et al., 2009, MNRAS, 394, 995
Dupret M. A., 2001, A&A, 366, 166
Dupret M., Grigahcène A., Garrido R., Gabriel M., Scuflaire R., 2004, A&A, 414, L17
Dziembowski W., 1977, Acta Astron., 27, 95
Gilliland R. L. et al., 2010, ApJ, 713, L160
Goupil M.-J., Dupret M. A., Samadi R., Boehm T., Alecian E., Suarez J. C., Lebreton Y., Catala C., 2005, J. Astrophys. Astron., 26, 249
Grevesse N., Asplund M., Sauval A. J., Scott P., 2010, Ap&SS, 328, 179
Grigahcène A., Dupret M.-A., Gabriel M., Garrido R., Scuflaire R., 2005, A&A, 434, 1055
Grigahcène A. et al., 2010, ApJ, 713, L192
Guzik J. A., Kaye A. B., Bradley P. A., Cox A. N., Neuforge C., 2000, ApJ, 542, L57
Jenkins J. M. et al., 2010, ApJ, 713, L120
Jin H., Kim S., Kwon S., Youn J., Lee C., Lee D., Kim K., 2003, A&A, 404, 621
Koch D. G. et al., 2010, ApJ, 713, L79
Kurucz R. L., 1993, ATLAS9 Stellar Atmosphere Programs and 2 km/s Grid. Kurucz CD-ROM No. 13. Smithsonian Astrophysical Observatory, Cambridge, MA
Kurucz R. L., Avrett E. H., 1981, SAO Special Report No. 391
Kurucz R. L., Bell B., 1995, Atomic Line Data. Kurucz CD-ROM No. 23. Smithsonian Astrophysical Observatory, Cambridge, MA
Lee Y., Kim S. S., Shin J., Lee J., Jin H., 2008, PASJ, 60, 551
Lenz P., Pamyatnykh A. A., Breger M., Antoci V., 2008, A&A, 478, 855
Lignières F., Rieutord M., Reese D., 2006, A&A, 455, 607
McNamara D. H., 2000, in Breger M., Montgomery M., eds, ASP Conf. Ser. Vol. 210, Delta Scuti and Related Stars. Astron. Soc. Pac., San Francisco, p. 373
Marconi M., Palla F., 1998, ApJ, 507, L141
Morel P., 1997, A&AS, 124, 597
Morel P., Lebreton Y., 2008, Ap&SS, 316, 61
Moya A., Garrido R., Dupret M. A., 2004, A&A, 414, 1081
Mulet-Marquis C., Glatzel W., Baraffe I., Winisdoerffer C., 2007, A&A, 465, 937
Petersen J. O., 1973, A&A, 27, 89
Pigulski A., Pojmański G., Pilecki B., Szczygieł D. M., 2009, Acta Astron., 59, 33
Poretti E., 2003, A&A, 409, 1031
Poretti E. et al., 2005, A&A, 440, 1097
Poretti E. et al., 2009, A&A, 506, 85
Poretti E. et al., 2011, A&A, 528, A147
Reese D., Lignières F., Rieutord M., 2008, A&A, 481, 449
Reese D. R., MacGregor K. B., Jackson S., Skumanich A., Metcalfe T. S., 2009a, A&A, 506, 189
Reese D. R., Thompson M. J., MacGregor K. B., Jackson S., Skumanich A., Metcalfe T. S., 2009b, A&A, 506, 183
Rodríguez E., López-González M. J., López de Coca P., 2000, A&AS, 144, 469
Rodríguez E., Laney C. D., Amado P. J., Lopez-Gonzalez M. J., Joner M., 2004, Commun. Asteroseismol., 145, 48
Scuflaire R., Montalbán J., Théado S., Bourge P.-O., Miglio A., Godart M., Thoul A., Noels A., 2008a, Ap&SS, 316, 149
Scuflaire R., Théado S., Montalbán J., Miglio A., Bourge P.-O., Godart M., Thoul A., Noels A., 2008b, Ap&SS, 316, 83
Soszynski I. et al., 2008, Acta Astron., 58, 163
Soufi F., Goupil M. J., Dziembowski W. A., 1998, A&A, 334, 911
Stellingwerf R. F., 1982, ApJ, 262, 330
Suárez J. C., Bruntt H., Buzasi D., 2005, A&A, 438, 633
Suárez J. C., Garrido R., Goupil M. J., 2006, A&A, 447, 649
Suárez J. C., Garrido R., Moya A., 2007, A&A, 474, 961
Suran M. D., 2008, Ap&SS, 316, 163
Torres G., Andersen J., Giménez A., 2010, A&AR, 18, 67
Uytterhoeven K. et al., 2011, A&A, 534, A125
Ventura P., Zeppieri A., Mazzitelli I., D'Antona F., 1998, A&A, 334, 953
Walraven T., Walraven J., Balona L. A., 1992, MNRAS, 254, 59

This paper has been typeset from a TEX/LATEX file prepared by the author.

Downloaded from http://mnras.oxfordjournals.org/ by guest on March 17, 2016